Pergamon

SCIENCE DIRECT®

Bioorganic & Medicinal Chemistry Letters 13 (2003) 4093–4100

BIOORGANIC & MEDICINAL CHEMISTRY LETTERS

Interaction of the Disodium Disuccinate Derivative of *meso*-Astaxanthin with Human Serum Albumin: From Chiral Complexation to Self-Assembly

Ferenc Zsila,[a] Miklós Simonyi[a] and Samuel F. Lockwood[b,*]

[a]*Department of Molecular Pharmacology, Institute of Chemistry, Chemical Research Center, PO Box 17, H-1525 Budapest, Hungary*

[b]*Hawaii Biotech, Inc., 99-193 Aiea Heights Drive, Suite 200, Aiea, HI 96701, USA*

Received 24 June 2003; revised 11 August 2003; accepted 13 August 2003

Abstract—To exploit the promising biochemical activities of naturally-occurring and synthetic hydrophobic carotenoids, it is necessary to improve their aqueous solubility. The disodium disuccinate derivative of synthetic *meso*-astaxanthin was prepared, and its behavior in pH 7.4 buffer solutions in both the presence and absence of fatty acid-free human serum albumin (HSA) was evaluated. The induced circular dichroism (CD) spectra and red-shifted absorption band of the optically inactive ligand as well as the fluorescence quenching of HSA indicated that at low ligand/protein ratios (less than approximately 1:1 ligand/protein), the *meso*-carotenoid bound to albumin in monomeric form. Based on the current experimental and available structural data for HSA, the binding site was tentatively localized to the large interdomain cleft of HSA. Around a 1:1 *meso*-carotenoid/HSA molar ratio, characteristic positive-negative bands appeared in the visible region of the CD spectrum, whose amplitudes increased in parallel with the increasing concentration of the ligand. These oppositely-signed Cotton effects are typical for chiral intermolecular exciton coupling between adjacent polyene chains arranged in right-handed assembly. Surprisingly, the magnitude of these induced CD bands continued to increase at high ligand/protein ratios (up to 13:1 *meso*-carotenoid/HSA). These results suggest the formation of unique, mixed-type carotenoid–albumin assemblies in which the HSA molecules themselves serve as chiral templates for the generation of supramolecular assemblies.

The naturally-occurring carotenoids are a related group of greater than 600 compounds, exclusive of stereo- and geometric isomers, with demonstrated potent antioxidant capacity.[1] The family of carotenoids is divided into hydrocarbon carotenoids ('carotenes') and oxygen-substituted carotenoids ('xanthophylls'). The natural compounds are excellent singlet oxygen quenchers as well as lipid peroxidation chain-breakers; as such, they share this dual antioxidant capability with vitamin E. As the number of conjugated double bonds along the polyene chain length increases, the singlet oxygen quenching ability correspondingly increases.[2] Lycopene—the carotene endowing tomatoes and watermelon with their bright red colors—typically demonstrates the greatest singlet oxygen quenching capacity when compared in model systems with other carotenoids.[3] Lycopene shares with γ-carotene, astaxanthin, and canthaxanthin a total of 11 conjugated C=C double bonds. However, the poor aqueous solubility of most carotenes, and the vast majority of xanthophylls limits their use as aqueous-phase singlet oxygen quenchers and radical scavengers. Chemical modifications which increase the apparent solubility and/or dispersibility of the carotenoids have found application in basic science as well as clinical research.[4] However, the tendency for the parent carotenoids and novel derivatives to form supramolecular assemblies in aqueous solution warrants comprehensive evaluation of such behavior prior to moving into in vitro and in vivo assays of the efficacy of such compounds.[5–7]

Hawaii Biotech, Inc. (HBI) successfully synthesized a novel carotenoid derivative, the disodium disuccinate derivative (dAST) of synthetic *meso*-astaxanthin (3*R*,3′*S*-dihydroxy-β,β-carotene-4,4′-dione), in all-*trans* (all-*E*) form (Fig. 1). The symmetric C_{40}-xanthophyll

*Corresponding author. Tel.: +1-808-2209168; fax: +1-808-4877341; e-mail: slockwood@hibiotech.com

0960-894X/$ - see front matter © 2003 Elsevier Ltd. All rights reserved.
doi:10.1016/j.bmcl.2003.08.026

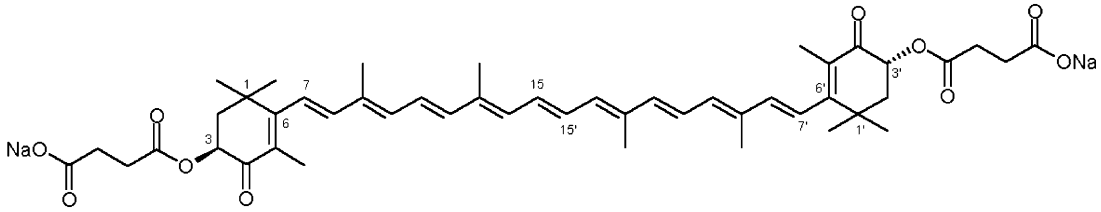

Figure 1. Chemical structure of the all-*trans* (all-*E*) disodium disuccinate ester derivative of *meso*-astaxanthin (3*R*,3′*S*- or 3*S*,3′*R*-dihydroxy-β,β-carotene-4,4′-dione; dAST) synthesized for the current study (shown as the all-*E* dianionic bolaamphiphile).

used to generate the new derivative has two chiral centers at the 3- and 3′- positions, but it exhibits optical activity neither in organic nor aqueous solutions, as these stereocenters have opposite absolute configurations and internally compensate each other.[8] As has been demonstrated in our earlier work,[9] natural carotenoid molecules possessing carboxylic functionality bind preferentially to human serum albumin (HSA), the most abundant protein in the blood.[10] Since albumin binding strongly influences the potential in vivo biochemical activities of a given compound,[10–12] we used circular dichroism (CD), ultraviolet–visible (UV–vis) and fluorescence spectroscopy to characterize the interaction of this novel carotenoid derivative with fatty acid-free HSA. To the authors' knowledge, this is the first investigation of the protein binding and aggregation properties of a symmetric carotenoid attached through direct esterification to a moiety with carboxylate end groups, forming a rigid, long-chain, highly unsaturated dianionic bolaamphiphile. It was verified that in buffer solution in the absence of protein, the *meso*-carotenoid formed closely-packed H-type (card-pack) aggregates[13] exhibiting no CD Cotton effects (CE). At low ligand/protein (L/P) molar ratios, however, the meso-carotenoid immediately and preferentially associated with HSA in monomeric fashion, suggesting that the secondary chemical interactions (van der Waals forces, hydrogen bonding) that permit supramolecular assembly in aqueous solution were overcome in a biologically relevant environment. Above 1:1 ligand/protein molar ratio the *meso*-carotenoid molecules again began to aggregate; surprisingly, the aggregation observed at these ratios was chiral, resulting in a supramolecular structure showing intense, exciton-type CD activity,[7,13] a unique observation described here for the first time.

The novel derivative dAST was synthesized from crystalline astaxanthin [3*R*,3′*R*, 3*R*,3′*S*, 3*S*,3′*S* (25:50:25)], a statistical mixture of stereioisomers obtained commercially (Buckton-Scott, India). The astaxanthin stereoisomers were separated by high-pressure liquid chromatography (HPLC), allowing for the synthesis of the purified *meso*-disodium disuccinate derivative for testing in the current study. The all-*trans* (all-*E*) form of the meso stereoisomer used was a linear, rigid molecule owing to the lack of *cis* (or *Z*) configuration(s) in the polyene chain of the spacer material (Fig. 1). The disodium disuccinate derivative of synthetic *meso*-astaxanthin was successfully synthesized at >99% purity by HPLC. The synthetic and analytical methodologies utilized to manufacture this novel derivative will be published separately.

Materials

Essentially fatty acid-free human serum albumin (catalog No. A-1887, lot No. 14H9319) was obtained from Sigma and used as supplied. Double-distilled water and spectroscopy grade dimethyl sulfoxide (DMSO, Scharlau Chemie S.A., Barcelona, Spain) and ethanol (Chemolab, Budapest, Hungary) were used. All other chemicals were of analytical grade.

Preparation of stock solution of dAST

After dissolution of the *meso*-carotenoid in DMSO, 100 μL of DMSO solution was added to 2 mL ethanol in a rectangular cuvette with 1 cm pathlength. The absorption spectrum was registered between 260 and 650 nm. Concentration was calculated from the light absorption value at the λ_{max} ($\varepsilon_{478\ nm} = 116{,}570\ M^{-1}\ cm^{-1}$).[14]

Preparation of HSA solutions

For spectroscopic sample preparation, HSA was dissolved in pH 7.4 Ringer or 0.1 M pH 7.4 phosphate buffer solutions. Albumin concentration was calculated with the value of $E^{1\%}_{1\ cm} = 5.31$, using experimentally obtained absorbance data at 279 nm.[10] The molecular weight of HSA was defined as 66500 Da.[10,12]

Circular dichroism and UV–vis absorption spectroscopy

CD and UV-vis spectra were recorded on a Jasco J-715 spectropolarimeter at 25±0.2 and 37±0.2 °C in a rectangular cuvette with 1 cm pathlength. Temperature control was provided by a Peltier thermostat equipped with magnetic stirring. All spectra were accumulated three times with a bandwidth of 1.0 nm and a resolution of 0.5 nm at a scan speed of 100 nm/min. Induced CD was defined as the CD of the dAST–HSA mixture minus the CD of HSA alone at the same wavelengths, and is expressed as ellipticity in millidegrees (mdeg).

CD/UV–vis titration of HSA with dAST in pH 7.4 Ringer and 0.1 M phosphate buffer solutions at 37 °C

Ringer buffer, L/P values from 0.007 to 0.10. 2 mL of 1.6×10^{-4} M HSA solution was placed in the cuvette with 1 cm optical pathlength and small amounts of the ligand stock solution (*c* 2.2×10^{-4} M) were added with an automatic pipette in 10 μL aliquots.

Ringer buffer, L/P values from 0.82 to 13.13. 2 mL of 2.3×10^{-6} M HSA solution was placed in the cuvette with 1 cm optical pathlength and μL volumes of the

ligand stock solution (c 3.9×10^{-4} M) were added with an automatic pipette.

Phosphate buffer, L/P values from 0.82 to 13.10. 2 mL of 2.2×10^{-6} M HSA solution was placed in the cuvette with 1 cm optical pathlength and μL volumes of the ligand stock solution (c 3.6×10^{-4} M) were added with an automatic pipette.

Measurement of the intrinsic fluorescence of HSA in the presence of dAST

2 mL of 4.2×10^{-6} M HSA solution was prepared in a 1 cm rectangular cell in 0.1 M pH 7.4 phosphate buffer. 1.3×10^{-4} and 3.3×10^{-4} M *meso*-carotenoid DMSO solutions were consecutively added in μL volumes to the cuvette in the sample chamber of the Jasco J-715 spectropolarimeter. The resulting sample solution was excited between 240 and 360 nm in 0.5 nm wavelength increments. Total fluorescence intensity was collected at each wavelength with a Hamamatsu H5784-type photomultiplier detector mounted on a right angle to the light source.

In the sample solution, initial and final concentrations of HSA and dAST were 4.2×10^{-6}–4.0×10^{-6} M and 1.3×10^{-7}–1.4×10^{-5} M, respectively. The *meso*-carotenoid/HSA molar ratio was varied between 0.03 and 3.53. During the fluorescence measurements, final DMSO concentration did not exceed 5 v/v%. A control experiment was also performed, in which the fluorescence of HSA during addition of 20, 50 and 100 μL DMSO to the solution was measured.

UV–vis and CD spectral properties of dAST in ethanol and aqueous buffer solution

Because of its extended π-system, dAST exhibited intense light absorption in the visible spectrum (Fig. 2). The main bell-shaped absorption band centered at 481.5 nm was due to the lowest energy electronic dipole allowed, a π→π* transition polarized along the long axis of the polyene chain. At room temperature, lack of fine structure is typical for carotenoids containing one or more conjugated carbonyl groups. However, the vibrational sub-bands were indeed present beneath this curve, as revealed by the second derivative of the spectrum (Fig. 2). Additionally, in the near-UV region, further transitions were present. According to theoretical calculations performed on polyene models,[15] the electronic transition moment (μ) of the moderately intense band around 300 nm is polarized parallel to the long axis of the dAST molecule. At the same time, the band at 371 nm μ is oriented along the 2-fold, C_2 symmetry axis of the conjugated system. The weak n→π* transitions of the carbonyl groups were obscured by the other bands.[16] As expected, the *meso*-carotenoid compound did not show any CD bands in ethanol since the effects of the two opposite chiral centers (3*R*,3′*S*) canceled each other (data not shown).[8,17]

In Ringer buffer solution, the principal absorption band of dAST changed dramatically, exhibiting a large blue-shift (2541.6 cm^{-1}) as well as bandwidth narrowing (Fig. 3). These spectral changes indicated the formation of so-called 'card-pack' aggregates, in which the molecules were held together in close proximity (within a few angstroms) by both exclusion from the aqueous environment and H-bonding interactions.[7,18] As a result, the excited-state wave functions of the polyene chains were delocalized *inter*-molecularly, allowing exciton resonance interaction[6,13] to occur between neighbouring molecules. This interaction resulted in a high-energy exciton peak in the UV–vis spectrum. Due to unfavourable steric interactions arising among the bulky end-groups, parallel alignment of the polyene chains is not allowed; the long axes of the separate molecules instead close a definite intermolecular overlay angle.[7,13,18]

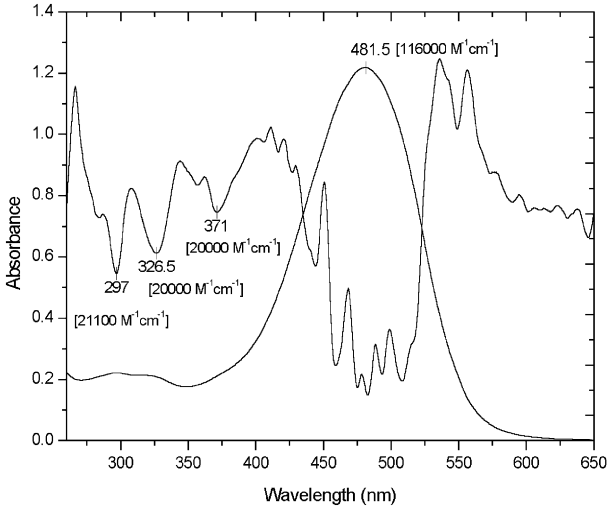

Figure 2. Ultraviolet-visible absorption spectrum of dAST in ethanol at 25 °C (cell length 1 cm, c 1.05×10^{-5} M). Molar absorption coefficients are shown in parentheses. The second derivative curve of the absorption spectrum indicates the exact position of peaks in the near-UV region and the hidden vibrational fine structure of the main band.

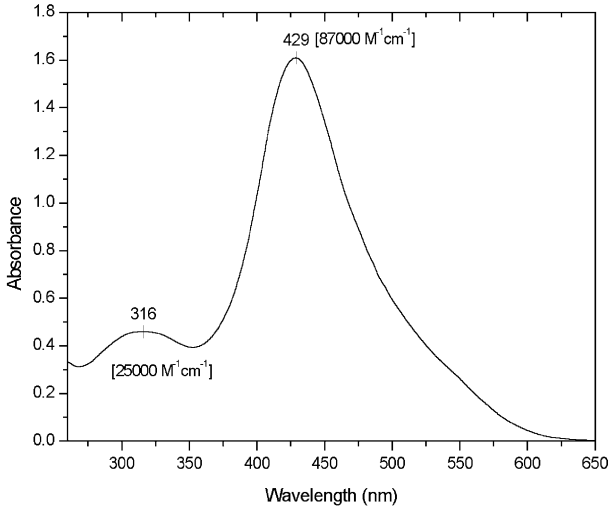

Figure 3. Absorption spectrum of dAST in Ringer buffer (pH 7.4, cell length 1 cm, c 1.85×10^{-5} M, $t=37$ °C). Molar absorption coefficients are indicated.

In such cases, carotenoid aggregates built up by chiral monomers also exhibit induced Cotton effects (CE) due to the chiral intermolecular arrangement determined by asymmetric centers. In contrast, the *meso*-carotenoid compound demonstrated no optical activity in the aggregated state in solution (data not shown) due to the lack of net chirality of the molecules.

Optical properties of dAST in the presence of human serum albumin at low ligand/protein molar ratios

Upon addition of dAST to the HSA solution prepared in pH 7.4 Ringer buffer, two definite, oppositely-signed induced CD bands appeared between 300 and 450 nm with a zero cross-over point at 367 nm (Fig. 4). The figure inserts show the intensities of the induced Cotton effects and the main absorption band at different L/P ratios ($\Delta\varepsilon$ and ε values are calculated with respect to the total *meso*-carotenoid concentration). Magnitudes of the CEs increased with increasing concentration of the ligand, however, their shape and wavelength positions remain unchanged. As mentioned above, there are two transitions below 450 nm which might be responsible for the observed optical activity.[15] The absorption band around 300 nm has transition symmetry B, and the corresponding electric and magnetic transition moments orientated along the polyene chain are perpendicular to the twofold symmetry axis. The electric and magnetic transition moments of the band at 372.5 nm are polarized parallel to the C_2 axis, its transition symmetry is A. It is reasonable to assume that upon protein binding, these bands shift to longer wavelengths due to the changing microenvironment surrounding the polyene chain. It has been well established that CD spectra of carotenoids in which the chromophoric portions belong to the C_2 point group conform to the C_2-rule:[15,19,20] if the overall conjugated system acquires right-handed chirality (i.e., dihedral angles around bonds 6–7 and 6′–7′ are negative), then transitions of symmetry A lead to negative CE, and transitions of symmetry B lead to positive CE (Fig. 4). Therefore, the *meso*-carotenoid binds to HSA in such a manner that the protein environment fixes the terminal rings in a well-defined chiral conformation that results in the observed negative- and positive-induced CD bands.

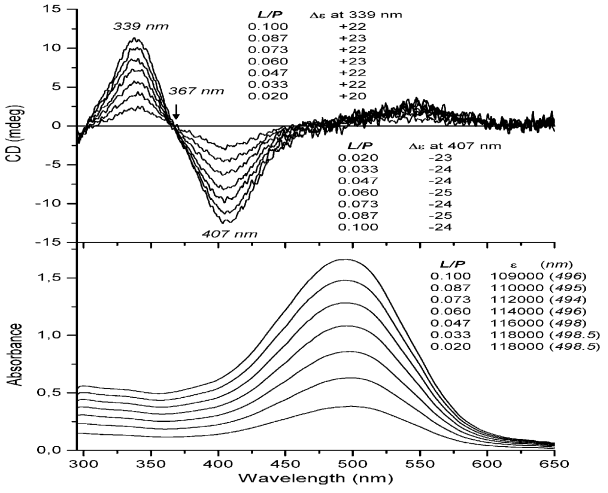

Figure 4. Induced CD and UV–vis spectra obtained by titration of HSA with dAST in Ringer buffer solution (pH 7.4) at low L/P ratios. Concentration of HSA was 1.6×10^{-4} M and the ligand was added as aliquots of DMSO stock solution (cell length 1 cm, $t=37\,^{\circ}C$). Curves measured at different L/P values are shown. Insets: molar circular dichroic absorption coefficients ($\Delta\varepsilon$ in M^{-1} cm^{-1}) and molar absorption coefficients (ε in M^{-1} cm^{-1}) of the induced CD and absorption bands calculated on the basis of total *meso*-carotenoid concentration in the solution.

It is worth mentioning that the absolute configurations of the chiral 3 and 3′ centers do not determine the chiroptical property of the molecule; rather, the asymmetric protein environment of the albumin molecule (via noncovalent chemical interactions) determines the observed activity. In contrast to the aggregate behavior in the aqueous solutions described above, the dAST molecules do not aggregate in HSA solution at these L/P ratios, as demonstrated by the retention of the bell-shaped and slightly red-shifted visible absorption band (Fig. 4). Thus, both the UV–vis absorption and CD spectra indicate that the binding of the *meso*-carotenoid molecules to HSA occurs in monomeric form.

Optical properties of dAST in the presence of HSA above 1:1 L/P ratios

An increasing amount of dAST was added to solutions of HSA prepared either with pH 7.4 Ringer or 0.1 M pH 7.4 phosphate buffer to achieve L/P ratios higher than 1. Both CD and UV–vis absorption spectra exhibited profound changes during addition of the ligand (Fig. 5a and b). In addition to the blue-shifted visible absorption band a new, positive-negative CD band pair appeared around 480 and 420 nm, respectively. These CE's exhibited no vibrational fine structure and their amplitudes grew with increasing concentration of the ligand. However, there were some notable differences between the spectra obtained in the Ringer and phosphate buffer solutions:

1. The main absorption band shifted to lower wavelength (434.5 nm) in Ringer buffer. The corresponding value was 451.5 nm in phosphate buffer.
2. Deviation of the zero cross-over point of CEs from the maximum of the absorption band was three times larger in Ringer (441.6 cm^{-1}) than phosphate buffer solution (148.4 cm^{-1}).
3. Above an L/P value of 8, the intensities of the CD bands no longer increased in Ringer solution. In contrast, the amplitude(s) of the CD bands continued to increase with increasing L/P ratio in phosphate buffer, even at an L/P value of 13.
4. At the same L/P ratios, more intense CD bands were measured in phosphate buffer (Fig. 5a and b).

The fact that these oppositely-signed CD bands appear only above 1:1 L/P ratio strongly suggests that they stemmed from chiral intermolecular interactions between adjacent *meso*-carotenoid molecules. When two electric transition dipole moments are similar in energy, lie close to each other in space, and form a chiral array, their interaction is manifested as chiral exciton coupling:

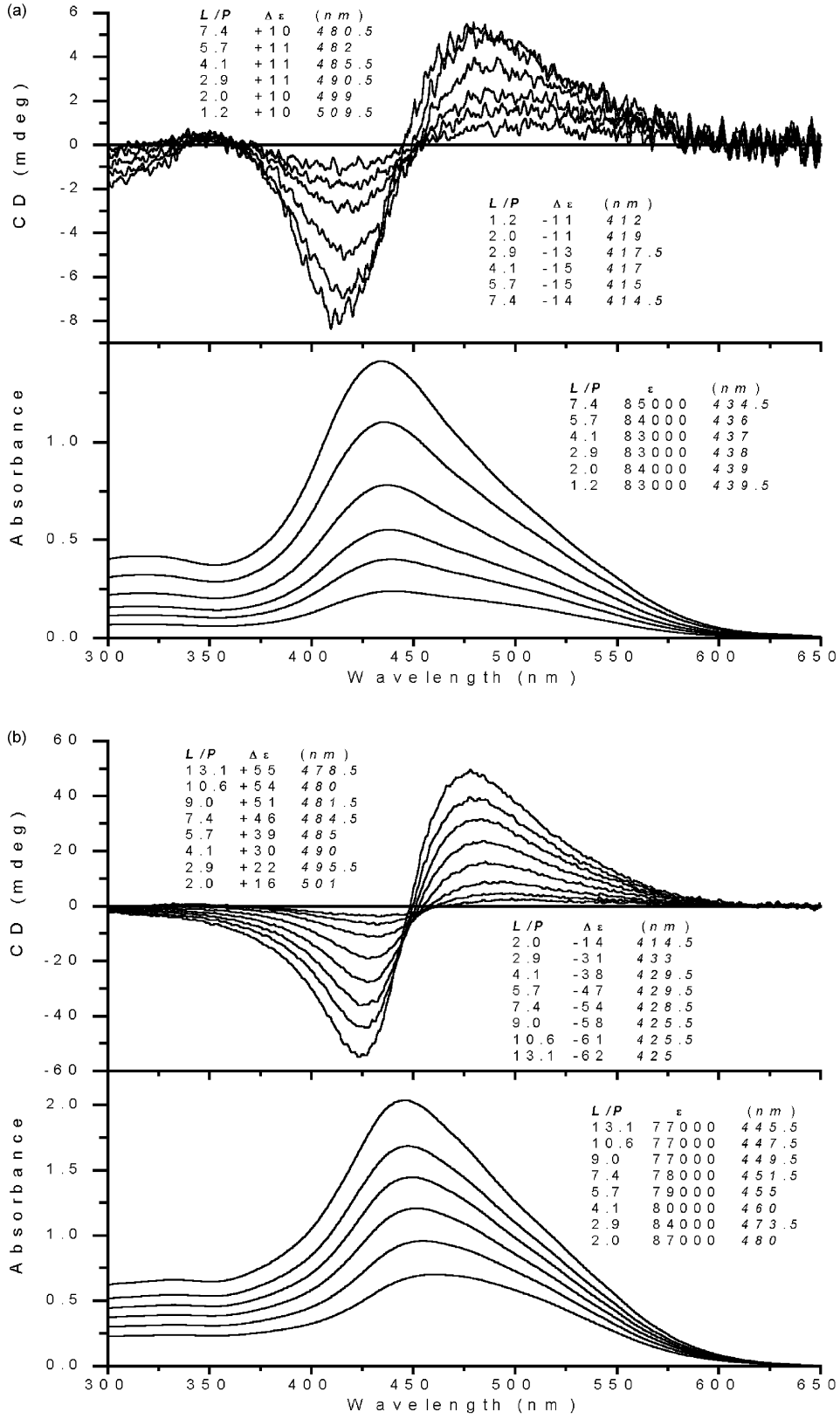

Figure 5. (a) Induced CD and UV–vis spectra obtained by titration of HSA with dAST in Ringer buffer solution (pH 7.4) above L/P ratio of 1. Concentration of HSA was 2.3×10^{-4} M and the ligand was added as aliquots of DMSO stock solution (cell length 1 cm, $t=37\,^{\circ}C$). Curves measured at L/P values of 1.2, 2.0, 2.9, 4.1, 5.7 and 7.4 are shown. CD intensities increase in parallel with the ligand concentration. (b) Induced CD and UV–vis spectra obtained by titration of HSA with dAST in 0.1 M pH 7.4 phosphate buffer solution above L/P ratio of 1. Concentration of HSA was 2.2×10^{-4} M and the ligand was added as aliquots of DMSO stock solution (cell length 1 cm, $t=37\,^{\circ}C$). Curves measured at L/P values of 2.0, 2.9, 4.1, 5.7, 9.0, 10.6 and 13.1 are shown. CD intensities increase in parallel with the ligand concentration.

the CD spectrum shows a bisignate couplet matched with the spectral position of the corresponding absorption band, whose sign is determined by the absolute sense of twist between the two dipoles.[21] According to the exciton chirality rule, a positive twist corresponds to a positive long-wavelength CE and a negative CE at shorter wavelength, and vice versa. In our case, the direction of the transition dipole moment is known; it is polarized along the long axis of the polyene chain. Thus, the neighboring *meso*-carotenoid molecules are arranged in such a manner that their long axes form a positive (clockwise) intermolecular overlay angle. Chiral arrangements of two conjugated chains shown in Figure 6 satisfy the former condition; in these cases, a long-wavelength positive and a short wavelength negative band would appear in the CD spectrum. However, the spectroscopic behavior of the absorption band helps to differentiate between these spatial arrangements. Due to unfavourable coulombic interactions between the transition dipole moments of neighbouring *meso*-carotenoid molecules in the case of (a) and (b) (Fig. 6), the absorption maximum shifts to higher energies (lower wavelengths); if the (c) form exists, then the absorption band widens and its maximum shifts to lower energies (higher wavelengths).[22] Consequently, dAST molecules form a right-handed chiral array in which the long axes of *meso*-carotenoid monomers form an acute, positive angle [Fig. 6(a) and (b)].

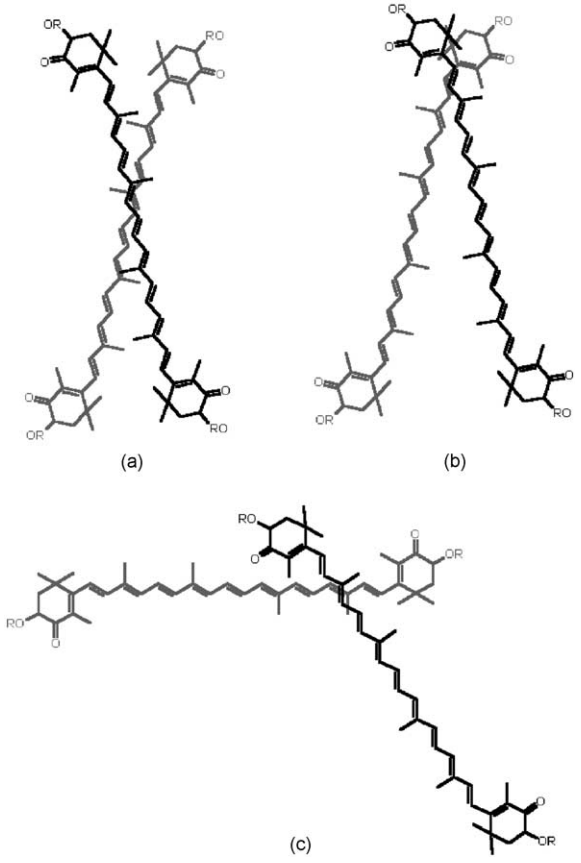

Figure 6. Illustration of right-handed chiral arrangements of two *meso*-carotenoid molecules for which excitonic interactions produce long-wavelength positive and short-wavelength negative cotton effects in the CD spectrum. Gray-colored molecules lie behind of the plane of the paper.

The following scenario is proposed for the origin of the chiral ordering of the ligand molecules. Albumin appears necessary for the induced optical activity and, at first, it is tempting to assume that there is a large binding site on HSA able to accommodate two *meso*-carotenoid molecules. At low L/P values albumin would bind only a single ligand; at higher L/P concentrations, a second *meso*-carotenoid monomer would be complexed. As stated above, however, the magnitudes of CEs continue to increase at quite high L/P values (Fig. 5b), in which case a single binding site should already be saturated. One resolution to this issue assumes that HSA is an asymmetric template on which the chiral self-assembly is started. The first few *meso*-carotenoid molecules bind to HSA in right-handed arrangement, and subsequent *meso*-carotenoid monomers build upon this chiral architecture. In this scenario, HSA provides the first essential step, the chiral initiation ('chiral seeding'); after this the self-assembly continues automatically. It is very important to note, however, that without their chiral end-groups only a few dAST molecules would be held in right-handed arrangement at the binding site of HSA. The 3 and 3′ chiral centers play a decisive role in allowing the aggregates to form the chiral self-assembly on the HSA molecules. In the absence of protein, the *meso*-carotenoid molecules form right- and left-handed assemblies to an equal extent, due to the lack of chiral discrimination.

As listed above, the spectral differences between the CD curves measured in phosphate buffer and Ringer solutions suggested the influence of the salt concentration on the stability of the aggregates (Fig. 5a and b). The osmolarity and ionic strength of the Ringer buffer was higher than that of phosphate buffer. The succinic moieties were ionized at pH 7.4 in both buffer solutions and electrostatic repulsion arose both within and among the aggregates. Positively-charged salt ions are able to decrease this repulsion, and therefore contribute to an increasing stability and size of the aggregates in the presence of these cations (Lockwood, unpublished results). During the titration of HSA with dAST above the 1:1 L/P ratio, both chiral and achiral aggregates were simultaneously formed; however, only chiral aggregates were associated with HSA, while achiral aggregates were not. CD spectra obtained in Ringer buffer solution (Fig. 5a) suggested that the achiral aggregates were better stabilized in this higher osmolarity buffer due to the screening effect of the salt ions. The added ligand molecules preferentially associated with existing aggregates, which resulted in the amplitudes of the CD bands reaching a plateau and becoming constant in contrast with the phosphate buffer.

Fluorescence quenching of HSA upon addition of dAST

The single tryptophan residue (Trp214) located in the depth of subdomain IIA is largely responsible for the intrinsic fluorescence of HSA.[10] The fluorescence emission spectrum of HSA overlaps with the absorption spectrum of the *meso*-carotenoid. Therefore, fluorescence spectroscopic measurements were performed during incremental addition of dAST in DMSO to a solution

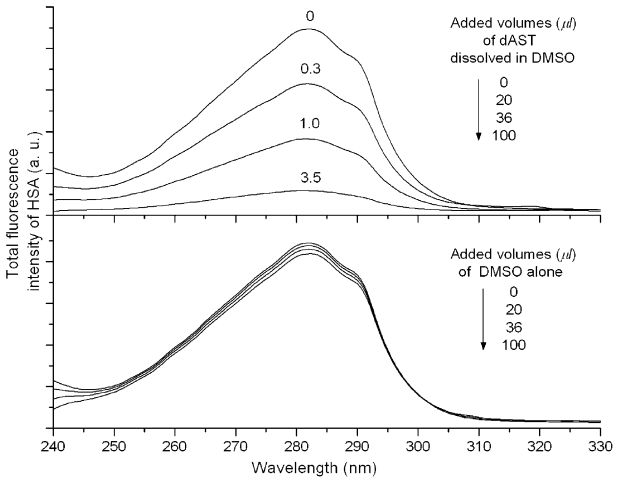

Figure 7. Upper figure: Fluorescence quenching of HSA by dAST measured in 0.1 M pH 7.4 phosphate buffer solution at 37 °C. Initial and final concentrations of HSA and the ligand were varied between 4.2×10^{-6}–4.0×10^{-6} M and 1.3×10^{-6}–1.4×10^{-5} M, respectively. L/P ratios are noted on curves. Lower figure: Effect of DMSO alone on the intrinsic flurescence of HSA. Experimental conditions are as above.

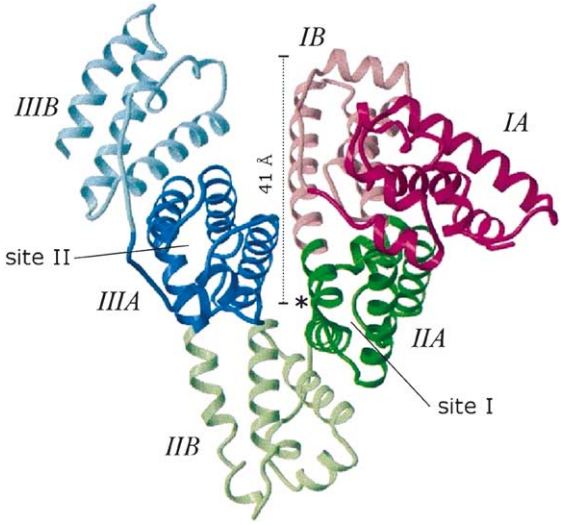

Figure 8. X-ray crystallographic structure of fatty acid-free HSA taken by permission from ref 24. Subdomains and the two primary drug-binding sites of HSA are indicated. Dotted bar represents spatial dimension of the interdomain cleft, and asterisk indicates the position of Trp214. The inter-atomic distance between the 3 and 3′ chiral carbon atoms of the dAST molecule is 28 Å.

of HSA. The results clearly demonstrated that the *meso*-carotenoid molecules were able to effectively quench the intrinsic fluorescence of HSA (Fig. 7). The DMSO used to prepare the stock solution of dAST exhibited a negligible effect on the intrinsic HSA fluorescence (Fig. 7). At an L/P ratio of 0.7, the baseline fluorescence intensity decreased by 50%. The observed phenomenon suggested that a *meso*-carotenoid molecule was bound in the vicinity of Trp214, which forms part of the wall in one of the two main drug-binding cavities of HSA (site I, subdomain IIA; Fig. 8). However, neither site I nor site II (subdomain IIIA) are capable of accommodating the long, rigid dAST molecule (Fig. 8).[23] Based on structural similarity, a second possibility is that dAST binds to long-chain (C18, C20) fatty acid binding sites of HSA, which have been well-characterized by high resolution X-ray crystallography.[24,25] In the case of shorter, open-chain carotenoids having no bulky end-groups, this possibility may be likely.[9] However, the polyene chain of the *meso*-carotenoid derivative itself measures 28 Å (between the 3 and 3′ chiral carbon atoms). Despite their conformational mobility, the succinate moieties require additional space, increasing the effective length of the molecule to 48 Å. Careful inspection of the crystal structure of HSA suggests that the long, narrow cleft between domains I and III may be suitable for the binding of a *meso*-carotenoid molecule (Fig. 8). The interdomain cleft is wide, and its narrow end is close to the tryptophan residue (Trp214; * in Fig. 8) which would provide a structural explanation for the observed fluorescence quenching.

As a consequence of exclusion from the aqueous environment and intermolecular hydrogen bonding, the disodium disuccinate derivative of synthetic, achiral *meso*-astaxanthin formed optically inactive, card-pack type aggregates in aqueous buffer solutions, as indicated by the large blue-shift of the main visible absorption band versus the band observed in ethanolic solution. In the presence of an excess of fatty acid-free HSA, the *meso*-carotenoid appears to be immediately and preferentially associated with HSA in monomeric fashion. These results suggest that the weak van der Waal's forces and hydrogen bonding that permits supramolecular assembly in aqueous solution will be rapidly overcome in a biologically relevant environment. The concentration of albumin in human blood in vivo is approximately 0.6 mM, suggesting that at doses of up to 500 mg, the *meso*-carotenoid (M_r 841 Da) will associate with the albumin in monomeric fashion (excluding additional potential non-specific binding to circulating blood cells and lipoproteins, which would increase the potential non-aggregating dose). Bound *meso*-carotenoid molecules exhibited induced CD bands which were adequately explained by a right-handed helical conformation of the conjugated system. Graded fluorescence quenching of HSA in the presence of increasing concentrations of dAST reinforced the notion that formation of carotenoid–albumin complexes were responsible for this quenching, and suggested spatial proximity between the bound ligand and the tryptophan 214 residue of HSA. Based on the spectroscopic data, the molecular length of the dAST molecule, and the well-characterized crystal structure of HSA, the binding site was tentatively assigned to the interdomain cleft located between domains I and III.

The authors also report for the first time the appearance of a positive-negative band pair in the CD spectrum above 1:1 L/P ratio of *meso*-carotenoid to HSA. This unusual finding was attributed to intermolacular chiral exciton coupling between *meso*-carotenoid polyene chains arranged in right-handed assembly. The experimental data suggested that HSA acts as a chiral template on which the self-assembly begins, and subsequently continues governed by the chirality of the end-groups of

the *meso*-carotenoid molecules. The differences between bisignate CD spectra obtained in pH 7.4 phosphate buffer and Ringer solutions indicate that the self-assembly is influenced by the osmolarity and ionic strength of the solution. With increasing osmolarity, the stability of the aggregates is enhanced presumably due to the electrostatic screening of the negatively-charged succinic carboxylate functions by salt cations.

References and Notes

1. Britton, G. *FASEB J*. **1995**, *9*, 1551.
2. Papas, A. M. *Mat. Med*. **1999**, November/December, 315.
3. Miki, W. *Pure Appl. Chem*. **1991**, *63*, 141.
4. Lockwood, S. F.; O'Malley, S.; Mosher, G. L. *J. Pharm. Sci*. **2003**, *92*, 922.
5. Buchwald, M.; Jencks, W. P. *Biochemistry* **1968**, *7*, 834.
6. Salares, V. R.; Young, N. M.; Carey, P. R.; Bernstein, H. J. *J. Raman Spectrosc*. **1977**, *6*, 282.
7. Zsila, F.; Bikádi, Z.; Deli, J.; Simonyi, M. *Chirality* **2001**, *13*, 446.
8. Müller, R. K.; Bernhard, K.; Mayer, H.; Ruttimann, A.; Vecchi, M. *Helv. Chim. Acta* **1980**, *63*, 1654.
9. Zsila, F.; Bikádi, Z.; Simonyi, M. *Tetrahedron: Asymmetry* **2001**, *12*, 3125.
10. Peters, T. *All About Albumin*; Academic: San Diego, 1996.
11. Watanabe, H.; Tanase, S.; Nakajou, K.; Maruyama, T.; Kragh-Hansen, U.; Otagiri, M. *Biochem. J*. **2000**, *349*, 813.
12. Kragh-Hansen, U.; Chuang, V. T.; Otagiri, M. *Biol. Pharm. Bull*. **2002**, *25*, 695.
13. Zsila, F.; Bikádi, Z.; Keresztes, Z.; Deli, J.; Simonyi, M. *J. Phys. Chem. B* **2001**, *105*, 9413.
14. Bernhard, K.; Englert, G.; Mayer, H.; Muller, R. K.; Ruttimann, A.; Vecchi, M.; Widmer, E.; Zell, R. *Helv. Chim. Acta* **1981**, *64*, 2469.
15. Sturzenegger, V.; Buchecker, R.; Wagniere, G. *Helv. Chim. Acta* **1980**, *63*, 1074.
16. Andrewes, A. G.; Borch, G.; Liaaen-Jensen, S.; Snatzke, G. *Acta Chem. Scand. B* **1974**, *28*, 730.
17. Lutnaes, B. F.; Gautun, O. R.; Liaaen-Jensen, S. *Chirality* **2001**, *13*, 224.
18. Bikádi, Z.; Zsila, F.; Deli, J.; Mády, G.; Simonyi, M. *Enantiomer* **2002**, *7*, 67.
19. Noack, K.; Thomson, A. *J. Helv. Chim. Acta* **1979**, *62*, 1902.
20. Noack, K.; Thomson, A. *J. Helv. Chim. Acta* **1981**, *64*, 2383.
21. Harada, N.; Nakanishi, K. *Circular Dichroic Spectroscopy - Exciton Coupling in Organic Stereochemistry*; University Science Books: Mill Valley, 1983.
22. Harada, N.; Takuma, Y.; Uda, H. *J. Am. Chem. Soc*. **1978**, *100*, 4029.
23. Choi, J. K.; Ho, J.; Curry, S.; Qin, D.; Bittman, R.; Hamilton, J. A. *J. Lipid Res*. **2002**, *43*, 1000.
24. Curry, S.; Brick, P.; Franks, N. P. *Biochim. Biophys. Acta* **1999**, *1441*, 131.
25. Petitpas, I.; Grune, T.; Bhattacharya, A. A.; Curry, S. *J. Mol. Biol*. **2001**, *314*, 955.